Research Article | Vol. 24, No. 22 | 31 Oct 2016 | OPTICS EXPRESS 25019

Optics EXPRESS

Photo-manipulated photonic bandgap devices based on optically tristable chiral-tilted homeotropic nematic liquid crystal

KUAN-CHUNG HUANG,[1] YU-CHENG HSIAO,[1] IVAN V. TIMOFEEV,[2,3] VICTOR YA. ZYRYANOV,[2] AND WEI LEE[1,*]

[1]*College of Photonics, National Chiao Tung University, Guiren Dist., Tainan 71150, Taiwan*
[2]*Kirensky Institute of Physics, Siberian Branch of the Russian Academy of Sciences, Krasnoyarsk 660036, Russia*
[3]*Laboratory for Nonlinear Optics and Spectroscopy, Siberian Federal University, Krasnoyarsk 660041, Russia*
**wlee@nctu.edu.tw*

Abstract: We report on the spectral properties of an optically switchable tristable chiral-tilted homeotropic nematic liquid crystal (LC) incorporated as a tunable defect layer in one-dimensional photonic crystal. By varying the polarization angle of the incident light and modulating the light intensity ratio between UV and green light, various transmission characteristics of the composite were obtained. The hybrid structure realizes photo-tunability in transmission of defect-mode peaks within the photonic bandgap in addition to optical switchability among three distinct sets of defect modes via photoinduced tristable state transitions. Because the fabrication process is easier and less critical in terms of cell parameters or sample preparation conditions and the LC layer itself possesses an extra stable state compared with the previously reported bistable counterpart operating on the basis of biased-voltage dual-frequency switching, it has much superior potential for photonic applications such as a low-power-consumption multichannel filter and an optically controllable intensity modulator.

OCIS codes: (160.3710) Liquid crystals; (160.1585) Chiral media; (160.4890) Organic materials; (230.3720) Liquid-crystal devices; (230.5298) Photonic crystals.

References and Links

1. E. Yablonovitch, "Inhibited spontaneous emission in solid-state physics and electronics," Phys. Rev. Lett. **58**(20), 2059–2062 (1987).
2. S. John, "Strong localization of photons in certain disordered dielectric superlattices," Phys. Rev. Lett. **58**(23), 2486–2489 (1987).
3. R. Ozaki, T. Matsui, M. Ozaki, and K. Yoshino, "Electro-tunable defect mode in one-dimensional periodic structure containing nematic liquid crystal as a defect layer," Jpn. J. Appl. Phys. **41**(Part 2, No. 12B), L1482–L1484 (2002).
4. P.-C. Wu and W. Lee, "Tunable and memorable optical devices with one-dimensional photonic-crystal/liquid-crystal hybrid structures," in *Optical Devices in Communication and Computation*, edited by Peng Xi (InTech, Croatia, September 19, 2012), Chap. 4, pp. 55–80.
5. Y.-T. Lin, W.-Y. Chang, C.-Y. Wu, V. Ya. Zyryanov, and W. Lee, "Optical properties of one-dimensional photonic crystal with a twisted-nematic defect layer," Opt. Express **18**(26), 26959–26964 (2010).
6. Y.-C. Hsiao, C.-Y. Wu, C.-H. Chen, V. Y. Zyryanov, and W. Lee, "Electro-optical device based on photonic structure with a dual-frequency cholesteric liquid crystal," Opt. Lett. **36**(14), 2632–2634 (2011).
7. Y.-C. Hsiao, C.-Y. Tang, and W. Lee, "Fast-switching bistable cholesteric intensity modulator," Opt. Express **19**(10), 9744–9749 (2011).
8. Y.-C. Hsiao, C.-T. Hou, V. Ya. Zyryanov, and W. Lee, "Multichannel photonic devices based on tristable polymer-stabilized cholesteric textures," Opt. Express **19**(24), 23952–23957 (2011).
9. A. Lorenz, R. Schuhmann, and H.-S. Kitzerow, "Switchable waveguiding in two liquid-crystal-filled photonic crystal fibers," Appl. Opt. **49**(20), 3846–3853 (2010).
10. D.-H. Ko, S. M. Morris, A. Lorenz, F. Castles, H. Butt, D. J. Gardiner, M. M. Qasim, B. Wallikewitz, P. J. W. Hands, T. D. Wilkinson, G. Amaratunga, H. J. Coles, and R. H. Friend, "A nano-patterned photonic crystal laser with a dye-doped liquid crystal," Appl. Phys. Lett. **103**(5), 051101 (2013).

#272044 http://dx.doi.org/10.1364/OE.24.025019
Journal © 2016 Received 25 Jul 2016; revised 13 Oct 2016; accepted 14 Oct 2016; published 18 Oct 2016

Optics EXPRESS

11. J.-C. Huang, Y.-C. Hsiao, Y.-T. Lin, C.-R. Lee, and W. Lee, "Electrically switchable organo-inorganic hybrid for a white-light laser source," Sci. Rep. **6**, 28363 (2016).
12. Y.-H. Lee, K.-C. Huang, W. Lee, and C.-Y. Chen, "Low-power displays with dye-doped bistable chiral-tilted homeotropic nematic liquid crystals," J. Disp. Technol. **10**(12), 1106–1109 (2014).
13. J.-S. Hsu, B.-J. Liang, and S.-H. Chen, "Bistable chiral tilted-homeotropic nematic liquid crystal cells," Appl. Phys. Lett. **85**(23), 5511–5513 (2004).
14. J.-S. Hsu, B.-J. Liang, and S.-H. Chen, "Dynamic behaviors of dual frequency liquid crystals in bistable chiral tilted-homeotropic nematic liquid crystal cell," Appl. Phys. Lett. **89**(5), 051920 (2006).
15. J.-S. Hsu, "Stability of bistable chiral-tilted homeotropic nematic liquid crystal displays," Jpn. J. Appl. Phys. **46**(11), 7378–7381 (2007).
16. B.-J. Liang, J.-S. Hsu, C.-L. Lin, and W.-C. Hsu, "Dynamic switching behavior of bistable chiral-tilted homeotropic nematic liquid crystal displays," J. Appl. Phys. **104**(7), 074509 (2008).
17. C.-Y. Wu, Y.-H. Zou, I. Timofeev, Y.-T. Lin, V. Ya. Zyryanov, J.-S. Hsu, and W. Lee, "Tunable bi-functional photonic device based on one-dimensional photonic crystal infiltrated with a bistable liquid-crystal layer," Opt. Express **19**(8), 7349–7355 (2011).
18. Y.-C. Hsiao, Y.-H. Zou, I. V. Timofeev, V. Ya. Zyryanov, and W. Lee, "Spectral modulation of a bistable liquid-crystal photonic structure by the polarization effect," Opt. Mater. Express **3**(6), 821–828 (2013).
19. Y.-C. Hsiao, K.-C. Huang, and Wei Lee, "Robust photo-switchable chiral liquid crystal with optical tristability enabled by a photoresponsive azo-chiral dopant," in preparation.
20. J. Ma, Y. Li, T. White, A. Urbas, and Q. Li, "Light-driven nanoscale chiral molecular switch: reversible dynamic full range color phototuning," Chem. Commun. (Camb.) **46**(20), 3463–3465 (2010).
21. C.-W. Chen, C.-C. Li, H.-C. Jau, C.-H. Lee, C. T. Wang, and T. H. Lin, "Bistable light-driven π phase switching using a twisted nematic liquid crystal film," Opt. Express **22**(10), 12133–12138 (2014).
22. J. Baudry, S. Pirkl, and P. Oswald, "Topological properties of singular fingers in frustrated cholesteric liquid crystals," Phys. Rev. E Stat. Phys. Plasmas Fluids Relat. Interdiscip. Topics **57**(3), 3038–3049 (1998).

1. Introduction

Photonic crystals (PCs) have allured much attention since two milestone papers were independently published in 1987 [1,2]. By inserting a third dielectric material as defect layer in a periodic structure comprising two alternating dielectric materials, defect modes are generated in the photonic bandgap (PBG). In 2002, Ozaki *et al*. first introduced a nematic liquid crystal (LC) as a defect layer in a one-dimensional (1-D) PC [3]. Based on the optical characteristics arising from the electrically tunable refractive index of LC bulks, various modes and forms of mesogenic materials have been studied in order to tune the spectral profile of the defect modes [4]. Lin and associates presented electrically tunable 1-D PC combining with a twisted-nematic defect layer [5]. Hsiao *et al*. revealed a bifunctional PC structure by adopting a dual-frequency (DF) cholesteric LC with bistable states as the defect layer [6,7]. Subsequently, they further developed a tristable multichannel device by infiltrating with polymer-stabilized cholesteric LC between two dielectric mirrors [8]. Moreover, the LC-filled PCs as fiber and tunable lasers have been also demonstrated in the past decade [9–11]. No matter how the PC technology progresses, the opto-optic tuning of PCs is highly desirable.

Recently, low-power-consumption devices have been vigorously pursued; LC memory devices boasting energy conservation have been proposed such as a reflective display using a dye-doped bistable chiral-tilted homeotropic nematic LC (BHN) system [12]. Stemming from the backflow effect in a chiral-doped DF LC characterized by frequency-revertible dielectric anisotropy, two optically bistable states, the tilted homeotropic (tH) and tilted twist (tT) states, electrically switch through the biased homeotropic (bH) and biased twist (bT) states [13–16]. In 2010, Wu *et al.* devised a 1-D PC incorporated with a BHN system as the central defect layer [17]. Later, Hsiao *et al*. further discussed the polarization effect on the spectral properties of the PC/BHN structure [18].

In this study, we present the transmission characteristics of an all-optical tunable photonic bandgap device based on a *tristable* chiral-tilted homeotropic nematic LC (THN) embedded in a 1-D PC [19]. The photo-switchable THN can switch directly and reversibly from one to another stable state without the need to transit through biased states (bH and bT) as required by the backflow mechanism. It is not only less critical in terms of sample preparation conditions such as the rubbing parameters, cell-gap-to-pitch-length ratio (d/p) or pretilt angle,

Optics EXPRESS

but also much advantageous by utilizing more readily available nematic LC instead of DF LC. Moreover, the system comparatively possesses an extra stable state in addition to the tH and tT state. Irradiated by two different light sources, the *trans–cis* photo-isomerization of the azo-chiral dopant takes place and, in turn, alters the additive's helical twisting power (HTP) [20] in the THN. Accordingly, one can adjust the intensity ratio of the UV to green light to control the chirality, thereby switching among the three optically stable states. In this study switching between E-mode and O-mode is also demonstrated in the single-polarizer scheme. Consequently, the photo-tunable grayscale system of PC/THN can be realized.

2. Experiment

THN was prepared by doping the photosensitive chiral bis(azobenzene) ChAD-3C-S (BEAM) at 0.33 wt% into the nematic host E7 (Merck), rendering an initial HTP of –42.6 μm^{-1} in the dark [21] and green-light-stabilized HTP of –30.7 μm^{-1}. The concoction was introduced into a 10-μm-thick empty cell consisting of two identical dielectric mirrors. Because of the spin-coated and antiparallel-rubbed alignment agent—a mixture of two polyimides, SE150 (planar alignment agent, Nissan) and AL-8395 (vertical alignment agent, Daily Polymer), the doped nematic took a pretilt angle of ~78° from the substrate plane, forming the chiral-tilted homeotropic nematic configuration [13]. Each dielectric mirror is made of a multilayer film—a periodic construction of alternate layers of Ta_2O_5 (n_H = 2.18) and SiO_2 (n_L = 1.47)—coated on an indium–tin-oxide glass substrate. The thicknesses of the Ta_2O_5 and SiO_2 layers are 68.09 nm and 102.37 nm, respectively, giving rise to a stopband centered at *ca.* 600 nm [17]. A schematic of the hybrid structure is shown in Fig. 1. The transmission spectra of the PC/THN were acquired under irradiation by both green and UV light. The green light source is an LED emitting at wavelength λ of 524 nm and the UV light derives from a UV LED (Panasonic UJ35) at λ = 365 nm. Both the green and UV sources deviate from the normal incidence by around 30° because of the spatial limitation. Throughout the experiment we fixed the intensity of green light, I_G, at 2.02 mW·cm^{-2} and adjusted the UV intensity I_{UV}. The transmission spectra of the PC/THN device were acquired with a fiber-optic spectrometer (Ocean Optics HR2000 +). The beam diameter is ~2 mm by employing a pinhole near the sample.

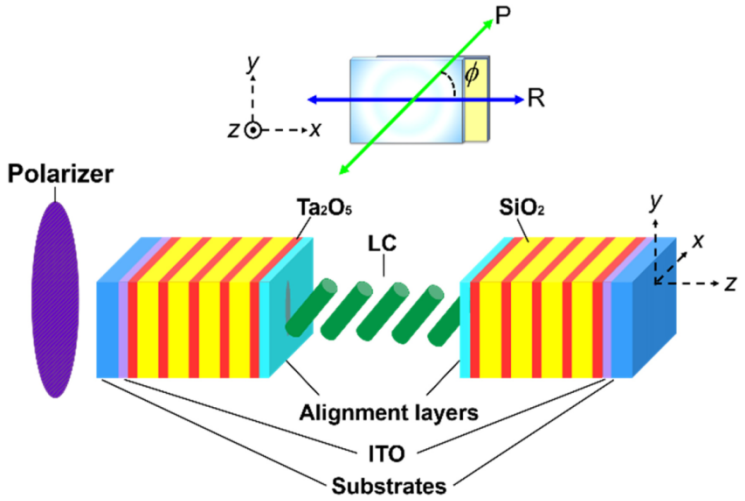

Fig. 1. Sandwich structure of the 1-D PC/THN construction. The arrows in the cell's front view indicate the transmission axis of the polarizer (P) as well as rubbing direction (R).

Optics EXPRESS

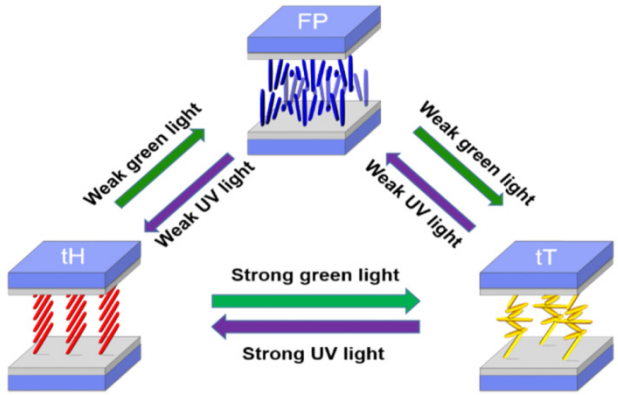

Fig. 2. Operating mechanisms of photo-induced THN in the tH, FP and tT states. The wavelengths of the UV and green light irradiation are 365 and 524 nm, respectively.

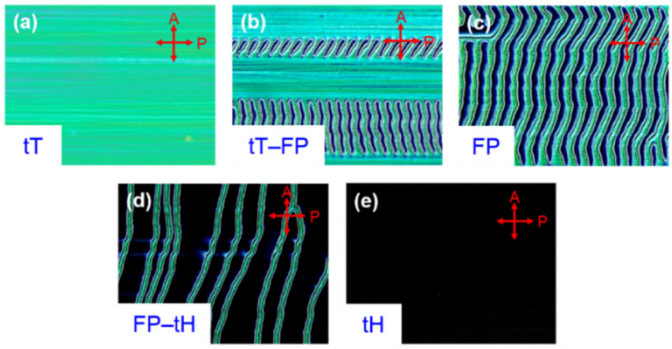

Fig. 3. The transition process among stable states under increasing irradiation ratios between UV and green light. (a) The tT state (I_{UV} = 0 mW·cm^{-2}); (b) the coexistence of tT and FP states (I_{UV} = 0.23 mW·cm^{-2}); (c) the FP state (I_{UV} = 0.41 mW·cm^{-2}); (d) the coexistence of FP and tH states (I_{UV} = 0.48 mW·cm^{-2}); (e) the pure tH state (I_{UV} = 0.57 mW·cm^{-2}) of a THN. The arrows indicate the transmission axes of the polarizer (P) and analyzer (A); the rubbing direction is along P.

3. Results and discussion

Figure 2 schematically depicts the optical switching mechanisms of THN among the tristable tH, fingerprint (FP), and tT states. We observed that the photo-induced unwinding converts the THN from the tT to tH state owing to the *tran–cis* isomerization of the chiral agent and the resulting reduction in LC chirality under irradiation by UV light (λ = 365 nm). It reverts to the tT state by exposure to green light (λ = 524 nm), but also transforms through the FP state—a scattering state—between tT and tH state with weak-intensity UV and green light irradiation. Under sufficient UV illumination, the azo chiral molecules isomerize to the *cis*-form and the HTP declines, resulting in a lengthened pitch greater than the threshold

$$P_{th} = 2d\frac{K_{22}}{K_{33}},$$

where d, K_{22} and K_{33} are the cell gap and the twist and bend elastic constants, respectively [22]. It can be inferred, therefore, in this condition that the twist torque becomes weak and the LC configuration favors the tH state due to the anchoring force on the treated surfaces. Oppositely, on illumination with green light, the azo chiral molecules recover the *trans*-form and, hence, the tT state. Interestingly, the cell is prone to the FP state, generated as an

Optics EXPRESS

intermediate stable state between tH and tT states when the HTP changes under the weak light illumination. Figure 3 shows the micrographic optical textures of the state-transform process among tT, FP, and tH states as observed under a crossed-polarizing optical microscope. Figures 3(a), 3(c), and 3(e) displays the tT state, FP state, and tH states, respectively. Note that the tH state looks completely dark in the crossed-polarizer scheme because $\varphi = 0$, meaning no birefringence can be observed.

Partial transmission spectra of defect modes within the PBG at various polarization angles ϕ are delineated in Fig. 4. Noticeably, the appearance of some companion defect modes and suppression of some defect peaks in the tH state and tT states are attributable to the birefringent splitting into two series of defect modes; namely, the E- and O-modes [5], for various polarization angles. In the tH state, the wavelengths of the defect modes at $\phi = 0°$ and $\phi = 90°$ are almost identical because the effective refractive index n_{eff} in the $\phi = 0°$ case is approximately equal to the ordinary refractive index n_o. It is clear from Fig. 4 that the transmittance of defect modes in the tH and tT states at $\phi = 90°$ is larger as compared with that at $\phi = 0°$. The damping, proportionally corresponding to the broadening, for the latter may originate from fluctuations of pretilt angle inside the light spot. Furthermore, the defect modes are polarization-independent of ϕ in the FP state due to the resulting strong scattering, giving minimal transmission to virtually regain the nature of a PBG. Obviously, these light combs with linewidths of *ca.* 1–3 nm in the tH and tT states can, therefore, switch to different wavelengths for the PC/THN to serve as a memory multichannel filter whereas cut off signals of light in the FP state like an optical shutter.

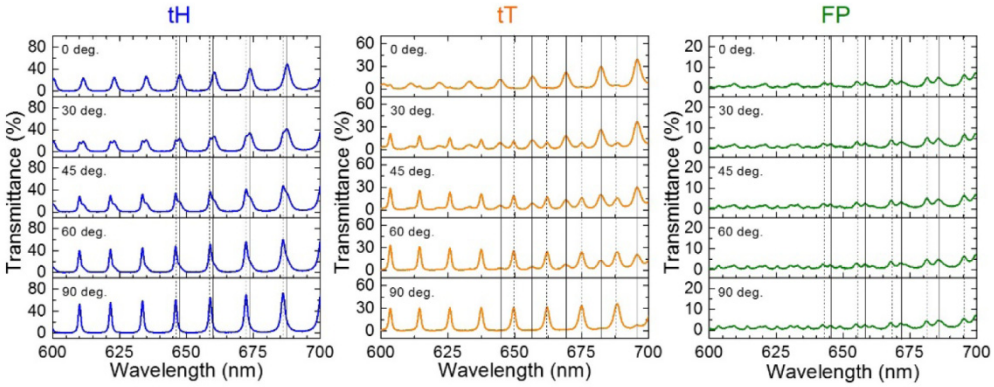

Fig. 4. Transmission spectra of defect modes between 600 and 700 nm in three stable states obtained at different polarization angles of incident light. A straight vertical line labels an E-mode wavelength whereas a dashed line labels an O-mode wavelength.

Optics EXPRESS

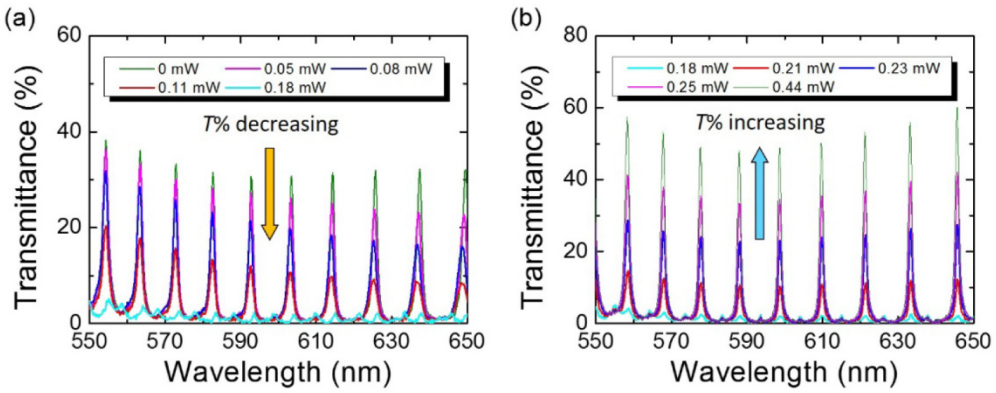

Fig. 5. Photo-manipulated transmittance of the defect modes under irradiation by green light (I_G = 2.02 mW/cm^2) as well as by various UV powers per unit area (i.e., cm^2). (a) From the tT to the FP state and (b) from the FP to tH state with increasing I_{UV}. Polarization angle ϕ = 90°.

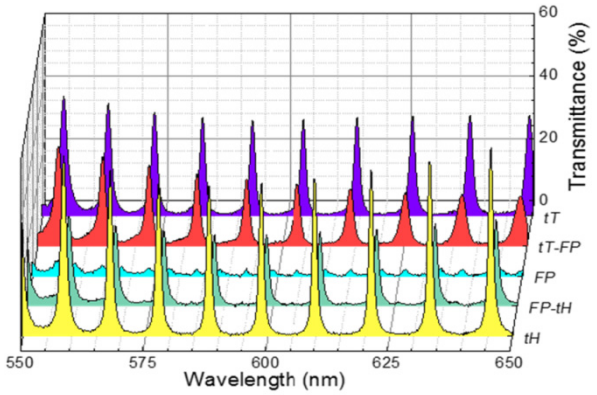

Fig. 6. The tunable and switchable characteristics of defect modes in different multiple stable states. The spectral data are retrieved from Fig. 5.

Figure 5 illustrates the transmittance modulation of defect-mode peaks by the UV light of various intensities when the green light radiance is fixed at 2.02 mW/cm^2. As can be seen in Fig. 5(a), the device remains in the tT state as I_{UV} = 0 mW/cm^2 due to the azo chiral dopant being stabilized in the *trans*-form. When I_{UV} increases gradually, *cis*-form dopant molecules also increases simultaneously. In line with the high-pretilt-angle and particular *d*/*p* conditions, the FP texture favorably appears. Then, one can see that the defect-mode peaks vanish because of strong scattering at I_{UV} = 0.18 mW/cm^2. With enhanced I_{UV}, the defect-mode peaks shift to distinct wavelengths and emerge again. When the azo chiral molecules become fully converted to the *trans*-form at 0.44 mW/cm^2, the cell reverts the tH state and the transmittance reaches the highest as shown in Fig. 5(b). Figure 6 provides an overview of typical defect-mode spectra in different states. It is evident that the scattering in the FP state effectively suppresses the transmittance of defect modes near the central wavelength of the PBG down to less than 1%. The transmission intensity of defect modes in both tH and tT states is dependent to the fluctuations of pretilt angle. The phenomenon is complicated and need the completely simulation results to support the explanation.

4. Conclusions

We succeed to demonstrate a novel concept of photo-switchable PC/THN devices. The device no longer requires a DF LC material and operates in a straightforward manner for photo-tuning among three optically stable states. In comparison with its bistable counterpart (BHN)

Optics EXPRESS

[13], THN can be prepared using a regular, readily available nematic host material (e.g., E7 in this study) and does not demand accurate fabrication conditions such as the rubbing parameter, *d*/*p* ratio and pretilt angle. The PC/THN device boasts its optical tristability and tunability in wavelength and transmittance of the defect modes via photo manipulation. The wavelength positions of these light channels can be switchable between E-mode and O-mode at different polarization angles. By adjusting the ratio of the UV to green light intensity, the defect peaks not only show a substantial variation in spectral amplitude through the stable FP state, but also can exhibit interleaved wavelength channels between the stable tT and tH states. This novel THN mode and the innovative mechanism for PC/THN devices should be fully developed for potential applications.

Funding

Ministry of Science and Technology (MOST), (103-2923-M-009-003-MY3); Ministry of Education and Science of the Russian Federation (3.1276.2014/K); Siberian Branch of the Russian Academy of Sciences under Complex Program II.2P (0358-2015-0010, 0358-2015-0011).